Cooperative Coverage Extension in Vehicular Land Mobile Satellite Networks

Giuseppe Cocco[‡], Nader Alagha[*] and Christian Ibars[†]

[‡]German Aerospace Center (DLR), Weßling, Germany

[*] European Space Agency, Noordwijk, The Netherlands

[†]CTTC, Barcelona, Spain

giuseppe.cocco@dlr.de, nader.alagha@esa.int, christian.ibars@cttc.es

Abstract

We study the application of random linear network coding (RLNC) for cooperative coverage extension in land mobile satellite (LMS) vehicular networks. We perform an analytical assessment of the limits of cooperation in the presence of both a satellite and a terrestrial repeater using the Max-flow Min-cut theorem and derive exact expressions for the general case as well as closed form lower bounds on the coverage in a setup of practical interest. Furthermore, we propose a practical implementation of the RLNC cooperative approach for the Digital Video Broadcasting - Satellite services to Handheld (DVB-SH) standard. We evaluate numerically the performance of the proposed protocol using a simulator based on physical layer abstraction and widely adopted propagation channel models for both the satellite and the terrestrial segment. Our simulation results show that the proposed scheme extends the coverage with respect to that of a system where simple relaying is used, making a more efficient use of the terrestrial channel resources, and can help to keep a relatively low outage probability while limiting the number of required terrestrial repeaters.

I. Introduction

In the last decade several proprietary solutions as well as open standards such as the DVB-SH [1] have been developed to enable data broadcasting via satellite to mobile users. Satellite broadcast and relaying capabilities give rise to the possibility of creating mobile broadcast systems over wide geographical areas, which opens large market opportunities for both handheld

DRAFT

and vehicular user terminals. Mobile broadcasting is of paramount importance for services such as digital TV or M2M communication, a new communication paradigm which will bring about a tremendous increase in the number of deployed wireless terminals [2].

Coverage, intended as the possibility for all nodes to correctly receive the data transmitted by a central node (e.g., a satellite or a base station), is a main issue for networks with a large number of terminals. As an example, such system could be used for navigation maps update in vehicle-mounted positioning systems or for terminal software and firmware update in M2M networks, where reliable broadcast transmission is of primary importance. Protocols such as ARQ, although very effective in point-to-point communication (see, e.g., [3, section 7.1.5]), may not be applicable in multicast contexts, since there may be many retransmission requests by the terminals in case of packets losses, which would saturate the return channel and overwhelm the source [4]. A cooperative approach may be applied in heterogeneous networks [2], in which terminals are equipped with both a long range (i.e., satellite reception) and a short range communication air interfaces.

A lot of work has been done on the use of cooperation [5] in multicast and broadcast communications in both terrestrial [6][7] and satellite networks [8][9][10]. Many of the proposed solutions [4][11][12], mainly regarding terrestrial networks, are based on network coding [13], that can achieve the Max-flow Min-cut capacity in ad-hoc networks. Cooperative content dissemination from road side units to vehicular networks based on rateless codes has also been studied in [14] and [15]. Lately the performance of different physical layer strategies for cooperative relaying in land mobile satellite (LMS) networks has been studied in [16], [17] and [18].

In the present paper we study the application of network coding for cooperative satellite coverage extension in LMS systems. Unlike in in [16], [17] and [18] we propose a solution that does not require any modification to the the physical and the data link layers of existing standards for LMS and vehicle-to-vehicle (V2V) communications and study the advantages of the proposed approach at system level. In the solution we present, the LMS and the V2V terminals, co-located in the vehicles, exchange information at an intermediate level between the data link and the network layer.

The present work extends and consolidates the preliminary results we presented in [19] and [20] by including the presence of terrestrial repeaters, also called *gap-fillers*, in both the analytical and the numerical study. In particular, we extend the results in [19] by building up a model which

is inspired by the Digital Video Broadcasting - Satellite services to Handheld (DVB-SH) [1] standard, where the same information is transmitted by the satellite and the terrestrial repeaters, constituting the complementary ground component (CGC), and combined at the physical layer by the user satellite terminal. The CGC is a system of fixed repeaters meant to provide coverage in those areas in which the satellite signals suffers deep shadowing caused by, e.g., tall buildings. Note that the combination of the signals from satellite and CGC is already foreseen in DVB-SH. We model the network as a directed graph in which the joint effect of the satellite and the gap-filler are taken into account through the statistics of the link between the source and the terminal. By applying the Max-flow Min-cut theorem and assuming Gaussian signalling under the hypothesis of block fading channels, we derive an exact expression for the outage probability as well as a closed-form lower bound for the case in which either the link from the satellite or that from the gap-filler suffers strong fading.

We support and complement the theoretical study with a numerical analysis based on the custom MATLAB/C++ - based simulator we developed. The enhancements with respect to [20] are the inclusion of a gap-filler, the implementation of the physical layer of IEEE 802.11p standard [21] (modulation, channel code and a simplified version of the channel access mechanism), the use of widely adopted channel models for the time series generation in the terrestrial channels [22] (both vehicle-to-vehicle and gap-filler-to-vehicle) and two key features of the DVB-SH-B standard, namely the physical layer combining of the signals received from the satellite and the CGC at the terminal nodes and the DVB-SH Raptor encoder/decoder [23]. All these features were not taken into account in [20]. The simulator interface between the physical channel and the protocol stack at higher layers leverages on Physical Layer Abstraction (PLA) [24] [25], which has been adopted in the standardization process of the IEEE 802.16 standard [26]. Several works [27] [28] showed that PLA allows to evaluate the link level performance of a system in a computationally affordable and with a good accuracy in different communication contexts. Our simulation results show that the proposed scheme extends the coverage with respect to a system where cooperation among vehicular terminals is implemented through simple relaying. The results also suggest that the cooperative approach can help to decrease the system outage probability while limiting the number of required terrestrial repeaters in areas characterized by challenging propagation conditions such as urban environments.

The rest of the paper is organized as follows. In Section II the system model is described. In Section III we study the non cooperative case, while in Section IV the proposed cooperative scheme is presented and analytical expressions for the coverage are derived. In Section V we introduce the DVB-SH standard, which is used as reference standard in Section VI, where a practical implementation of the cooperative approach is described. The proposed scheme implements the cooperative approach described in Section IV within the limits of existing standards. In Section VIII we describe the adopted simulation approach and the simulation setup, while in Section IX we present the numerical results. Finally, Section X contains the conclusions.

II. SYSTEM MODEL

A network is considered in which a source (S) has a set of K source messages $\mathbf{w}_1, \ldots, \mathbf{w}_K$ of k bits each, to broadcast to a population of M terminal nodes, each of which has both satellite reception (one-way communication) as well as short range communication (two-way, half duplex) capabilities. S delivers the data to the terminals through two relay nodes S_1 and S_2, i.e., there is no direct link between S and any of the terminals. The links between S and S_i, $i = 1, 2$, are assumed to be lossless [1]. S_1 and S_2 relay the data to the terminal nodes through orthogonal lossy wireless channels. With reference to DVB-SH-B, S_1 models a transparent satellite while S_2 models the fixed terrestrial repeater. In the rest of the paper we will use interchangeably the terms terrestrial repeater and gap-filler. The orthogonality is achieved in the frequency domain by allocating two disjoint frequency bands for the satellite and the gap-fillers. No feedback from the terminals or channel state information at the transmitter (CSIT) is assumed to S, S_1 and S_2, which implies a non-zero probability of packet loss. S_1 and S_2 protect each message using the same channel code (i.e., they transmit exactly the same signal) in order to decrease the probability of packet loss on the channel. A second level of protection is also applied by S at packet level in order to compensate for packet losses. The encoding at packet level takes place before the channel encoding. $N \geq K$ coded packets are created by S applying a random linear network code (RLNC) to the K source messages. We define $R = K/N$ as the rate of the NC

---

[1]in DVB-SH data is transmitted to the satellite through a high-throughput and highly reliable feeder link, while the distribution to the CGC network can take place either through a highly reliable satellite link or a terrestrial distribution network. Due to their high reliability such links are assumed as ideal, i.e., no packet loss occurs in the distribution network

encoder at S. Network coding operates in a finite field of size q ($GF(q)$), so that each message is treated as a vector of $k/\log_2(q)$ symbols. Source messages are linearly combined to produce encoded packets. An encoded packet $\mathbf{x}$ is generated as follows:

$$\mathbf{x} = \sum_{i=1}^{K} \varrho_i \mathbf{w}_i,$$

where ϱ_i, $i = 1, \ldots, K$ are random coefficients drawn according to a uniform distribution in $GF(q)$. The coefficients ϱ_i, $i = 1, \ldots, K$, are appended to each message $\mathbf{x}$ before its transmission. The set of appended coefficients represents the coordinates of the encoded message $\mathbf{x}$ in $GF(q)$ with respect to the basis $\{\mathbf{w}_i\}$, $i = 1, \ldots, K$, and is called *global encoding vector*.

The encoding at the physical layer is applied by S_1 and S_2 to network-encoded packets, each consisting of of k bits. S_1 and S_2 encode each packet using the same Gaussian codebook of size 2^{nr}, with $r = \frac{k}{n}$ bits per channel use (bpcu), associating a codeword $\mathbf{c}_m$ of n i.i.d. symbols drawn according to a Gaussian distribution to each $\mathbf{x}_m$, $m = 1 \ldots, N$ [3]. The time needed for S_1 and S_2 to transmit a packet is called *transmission slot (TS)*. Transmissions are synchronized in time such that symbols from the two orthogonal channels are aligned at the receiver [2].

The signals from S_1 and S_2 are combined at the physical layer using maximal-ratio combining. Terminals cooperate in order to recover the packets that are lost in the link from the transmitters. We assume terminals with high mobility, which is the case of, e.g., vehicular networks. Nodes have little time to set up connections with each other. For this, and in order to exploit the broadcast nature of the wireless medium, nodes act in *promiscuous mode*, broadcasting packets to all terminals within reach. Similarly as in the broadcast mode of IEEE 802.11p standard, no request to send (RTS)/clear to send (CTS) mechanism is assumed [29]. No CSIT is assumed at the transmitting terminal in the terrestrial communication, so that there is a non zero probability of packet loss. Unlike in 802.11p, each terminal uses two levels of encoding, one at the packet level and one at the physical level. The encoding procedure is detailed in the following.

Let L be the number of packets correctly decoded at the physical level by a terminal, received either through the satellite or the short range communication interface. The terminal selects the

[2]this is actually the case in DVB-SH-B, where synchronization can be kept between the satellite and the CGC such that symbol-level alignment can be achieved at the user terminals in case the same code rates and puncturing patterns are used in the two channels [1]. The different propagation delays from the CGC to terminals at different distances are compensated by the guard interval (GI) of the OFDM modulation in the terrestrial segment.

$L' \leq L$ packets which constitute the largest set of linearly independent packets with respect to the basis $\mathbf{w}_i$, $i = 1, \ldots, K$. Without loss of generality we assume that such set be $\mathbf{x}_1, \ldots, \mathbf{x}_{L'}$. Linear independence can be verified through the global encoding vectors of the packets. The L' selected packets are re-encoded together using RLNC, and then re-encoded at the physical layer. RLNC encoding at the terminals works as follows. Given the set of received packets $\mathbf{x}_1, \ldots, \mathbf{x}_{L'}$, the message $\mathbf{y} = \sum_{m=1}^{L'} \sigma_m \mathbf{x}_m$ is generated, σ_m, $m = 1, \ldots, L'$, being coefficients drawn at random according to a uniform distribution in $GF(q)$. Each time a new encoded message is created, it is appended its global encoding vector. The overhead this incurs is negligible if messages are sufficiently long [30]. The new global encoding vector η can be easily calculated by the transmitting node as follows:

$$\eta = \sigma \mathbf{\Psi},$$

where $\sigma = [\sigma_{\mathbf{1}} \; \cdots \; \sigma_{\mathbf{L'}}]$ is the *local encoding vector*, i.e., the vector of random coefficients chosen by the transmitting node, while $\mathbf{\Psi}$ is an $L' \times K$ matrix that has the global encoding vector of $\mathbf{x}_m$, $m = 1, \ldots, L'$, as row m. We assume that the transmission of a message by a terminal is completed within one TS. The physical layer encoding at a mobile node takes place in the same way as at the source, and using the same average transmission rate r.

A. Source-to-Node Channel Model

A Urban environment is assumed. We assume that channels from S_1 and S_2 to a given terminal N_i ($S_j - N$ channel, $j = 1, 2$) are affected by both Rayleigh fading and log-normal shadowing. The two channels are assumed to be statistically independent. The power of the signal received at the terminal from S_j, $j = 1, 2$ is modeled as the product of a unit-mean exponential random variable (r.v.) γ_j and a log-normal r.v. Γ_{S_j} which accounts for large scale fading. This model has been largely used to model propagation in urban scenarios [31] and, with some modifications, in LMS systems [32]. The fading coefficient γ_j takes into account the fast channel variations due to the terminal motion and is assumed to remain constant within a TS, while changing in an i.i.d. fashion at the end of each channel block. The shadowing coefficient Γ_{S_j} includes the transmitted power at S_j and accounts for path loss and obstruction caused by buildings in the line of sight and changes much slowly with respect to γ_j. For mathematical tractability we assume that Γ_{S_j} remains constant for N channel blocks, i.e., until all encoded packets relative

to the K source messages have been transmitted by S. In the following we will use the terms channel block and transmission slot interchangeably. We call the time needed to transmit N messages a *generation period (GP)*. The fading and shadowing processes of two different nodes and between the two different channels are assumed to be independent. We further assume that shadowing and fading statistics on each of the channels are the same for all nodes. We study the case of groups of terminals close enough to each other so that short-range communication can be used. We also assume that nodes are relatively far away from the gap-filler. Under these assumptions, the hypothesis of equal channel statistics across nodes can be regarded as a good approximation. The case of nodes close to the gap-filler is not relevant to our study and thus not explicitly considered. However, the mathematical results we derive implicitly take this case into account.

Due to the lack of CSIT there is a non zero probability that a message is not correctly decoded at each of the terminal nodes. This happens if the instantaneous channel capacity, assuming maximal-ratio combining, is lower than the transmission rate at the physical layer r. For ease of exposition we will refer to such channel as the S-N channel. Assuming the same channel statistics for all nodes, the packet loss probability in the S-N channel for any given node is:

$$P_{SN} = Pr\left\{\log_2(1 + \gamma_1 \Gamma_{S_1} + \gamma_2 \Gamma_{S_2}) < r\right\}, \tag{1}$$

where $\gamma_j \sim exp(1)$ while $\Gamma_{S_j} = e^{\frac{X_j}{10}}$, for $j = 1, 2$, with $X_j \sim \mathcal{N}(\mu_j, \sigma_j^2)$. Γ_{S_j} is constant within a GP, while γ_j changes independently at the end of each channel block. Fixing the values of Γ_{S_1} and Γ_{S_2}, the two random variables $\gamma_1' = \gamma_1 \Gamma_{S_1}$ and $\gamma_2' = \gamma_2 \Gamma_{S_2}$ are exponentially distributed with parameters $1/\Gamma_{S_1}$ and $1/\Gamma_{S_2}$, respectively. Using the fact that the sum $\gamma_1' + \gamma_2'$ in 1 has a hypoexponential distribution with parameters $1/\Gamma_{S_1}$ and $1/\Gamma_{S_2}$, we find the expression for the packet loss probability P_{SN} in the S-N channel:

$$P_{SN} = 1 - \frac{\Gamma_{S_1}}{\Gamma_{S_1} - \Gamma_{S_2}} e^{-\frac{2^r - 1}{\Gamma_{S_1}}} + \frac{\Gamma_{S_2}}{\Gamma_{S_1} - \Gamma_{S_2}} e^{-\frac{2^r - 1}{\Gamma_{S_2}}}. \tag{2}$$

In the rest of the paper we will use the expressions "packet loss rate" and "probability of packet loss" interchangeably. Due to shadowing, Γ_{S_1} and Γ_{S_2} change randomly and independently at each generation period and, within a generation, from one node to the other. Thus the packet loss rate P_{SN} is also a r.v. that remains constant within a generation and changes in an i.i.d. fashion across generations and terminals.

B. Node-to-Node Channel Model

We model the channels between the transmitting terminal and each of the receiving terminals (N-N channel) as independent block fading channels, i.e., the fading coefficient of each channel changes in an i.i.d. fashion at the end of each channel block. The probability of packet loss in the N-N channel P_{NN} is:

$$P_{NN} = Pr\left\{\log_2(1 + \gamma\Gamma_N) < r\right\} = 1 - e^{\frac{1-2^r}{\Gamma_N}}, \tag{3}$$

where Γ_N accounts for path loss and transmitted power, and is assumed to remain constant for a whole generation period and across terminals. In order not to saturate the terrestrial channel, we assume that a node can transmit at most one packet within one TS.

Note that expression (2) has been derived assuming that the same information is transmitted over both the satellite (S_1) and the gap-filler (S_2) links and the two signals are combined by the terminal nodes at the physical level. Since (3) grasps the effect of both links it allows to simplify the equivalent network topology by removing the intermediate nodes S_1 and S_2 as shown in the example of Fig. 1.
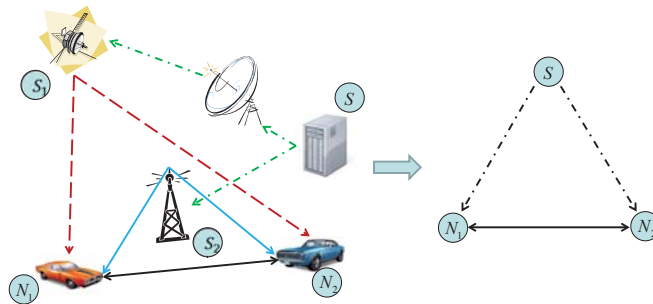

Fig. 1. Example of physical network (left) and the corresponding graph representation (right). The effect of the links from S_1 and S_2 in the physical network is taken into account in the SN link in the graph model by means of the packet loss rate given by Eqn. (2).

III. NON-COOPERATIVE COVERAGE

Let us consider a network with a source S and M terminals. We define the *coverage* (Ω) as the probability that all M terminals correctly decode the whole set of K source messages.

Assuming that K is large enough, and using the results in [4], the probability that a given node N can decode all the K source messages of a given generation in case of no cooperation is:

$$Pr\left\{P_{SN} < 1 - R\right\}, \tag{4}$$

$R = K/N$ being the rate of the NC encoder at S. We recall that, due to the shadowing, the packet loss rate P_{SN} is a r.v. which changes in an i.i.d. fashion across generations and terminals. The coverage is the probability that each of the nodes decodes all source messages, that is:

$$\Omega = Pr\left\{P_{SN1} < 1 - R, \ldots, P_{SNM} < 1 - R\right\}, \tag{5}$$

where P_{SNi} is the packet loss rate in the S-N link of node N_i, $i = 1, \ldots, M$. Under the assumption of i.i.d. channels we have $F_{P_{SNi}} = F_{P_{SN}}$, $\forall i \in \{1, \ldots, M\}$. Thus, (5) can be written as:

$$\begin{aligned}
\Omega &= \left(Pr\left\{P_{SN} < 1 - R\right\}\right)^M \\
&= \left(Pr\left\{1 - \frac{\Gamma_{S_1}}{\Gamma_{S_1} - \Gamma_{S_2}}e^{-\frac{2^r-1}{\Gamma_{S_1}}} + \frac{\Gamma_{S_2}}{\Gamma_{S_1} - \Gamma_{S_2}}e^{-\frac{2^r-1}{\Gamma_{S_2}}} < 1 - R\right\}\right)^M \\
&= \left(Pr\left\{\frac{\Gamma_{S_1}}{\Gamma_{S_1} - \Gamma_{S_2}}e^{-\frac{2^r-1}{\Gamma_{S_1}}} - \frac{\Gamma_{S_2}}{\Gamma_{S_1} - \Gamma_{S_2}}e^{-\frac{2^r-1}{\Gamma_{S_2}}} > R\right\}\right)^M.
\end{aligned} \tag{6}$$

Finding a closed form expression for Eqn. (6) for the general case is a challenging task since Γ_{S_1} and Γ_{S_2} are lognormal random variables with parameters (μ_1, σ_1) and (μ_2, σ_2), respectively. However, in Theorem 1 we derive a closed form expression in case either $\mu_1 \to \infty$ or $\mu_2 \to \infty$. Note that these are cases of practical interest since they correspond to a situation in which either the signal from the satellite or that from the gap-filler are faintly weak, which is the case of rural areas and dense urban areas, respectively.

Theorem 1: For any nonzero ϵ_μ, ϵ_{σ_i} and ϵ_{σ_j} if $0 < \epsilon_\mu < \mu_i < \infty$, $0 < \epsilon_{\sigma_i} < \sigma_i < \infty$, $0 < \epsilon_{\sigma_j} < \sigma_j < \infty$, $i \neq j$, then

$$\lim_{\mu_j \to -\infty} Pr\left\{\frac{\Gamma_{S_1}}{\Gamma_{S_1} - \Gamma_{S_2}}e^{-\frac{2^r-1}{\Gamma_{S_1}}} - \frac{\Gamma_{S_2}}{\Gamma_{S_1} - \Gamma_{S_2}}e^{-\frac{2^r-1}{\Gamma_{S_2}}} > R\right\} = \frac{1}{2} - \frac{1}{2}\text{erf}\left(\frac{10\ln\left[\frac{1-2^r}{\ln(R)}\right] - \mu_i}{2\sigma_i^2}\right) \tag{7}$$

Proof See the Appendix.

Note that, fixing R and M, the expression in Eqn. (7) goes to 0 as the rate at physical level r goes to infinity. This confirms the intuition according to which in the non-cooperative case

the coverage decreases as the transmission rate increases. As said previously, this result holds for any value of q as long as K is large enough. Thus, Eqn. (7) can also be interpreted as the coverage in a network of M nodes in presence of fading and shadowing that can be achieved for a rate couple (r, R) by a fountain code such as, e.g., a Raptor code.

IV. COOPERATIVE COVERAGE

The wireless network is modeled as a directed hypergraph $\mathcal{H} = (\mathcal{N}, \mathcal{A})$, $\mathcal{N}$ being a set of nodes and $\mathcal{A}$ a set of hyperarcs. A hyperarc is a pair (i, J), where i is the *head* node of the hyperarc while J is the subset of $\mathcal{N}$ connected to the head through the hyperarc. J is also called *tail*. A hyperarc (i, J) can be used to model a broadcast transmission from node i to nodes in J. Packet losses can also be taken into account. We want to study the relationship between the coverage and the rate at which the information is transferred to mobile terminals, which depends on both the rate at physical level r and the rate at which new messages are injected in the network, which is the rate at packet level R. In [4] (Theorem 2) it is shown that, if K is large, random linear network coding achieves the network capacity in wireless multicast connections, even in case of lossy links, if the number of innovative packets transmitted by the source per unit of time is lower than or equal to the flow across the minimum flow cut between the source and each of the sink nodes, i.e.:

$$R \leq \min_{Q \in \mathcal{Q}(S,t)} \left\{ \sum_{(i,J) \in \Gamma_+(Q)} \sum_{T \nsubseteq Q} z_{iJT} \right\} \tag{8}$$

where z_{iJT} is the average injection rate of packets in the arcs departing from i to the tail subset $T \subset J$, $\mathcal{Q}(S, t)$ is the set of all cuts between S and t, and $\Gamma_+(Q)$ denotes the set of forward hyperarcs of the cut Q, i.e.:

$$\Gamma_+(Q) = \{(i, J) \in \mathcal{A} | i \in Q, J \setminus Q \neq 0\}. \tag{9}$$

In other words, $\Gamma_+(Q)$ denotes the set of arcs of Q for which the head node is on the same side as the source, while at least one of the tail nodes of the relative hyperarc belongs to the other side of the cut. The rate z_{iJT} is defined as:

$$z_{iJT} = \lim_{\tau \to \infty} \frac{A_{iJT}(\tau)}{\tau}, \tag{10}$$

where $A_{iJT}(\tau)$ is the counting process of the packets sent by i that arrive in $T \subset J$ in the temporal interval $[0, \tau)$. The existence of an average rate is a necessary condition for the applicability of

the results in [4]. In the following we derive z_{iJT} for the considered network setup as a function of both physical layer and MAC layer parameters such as transmission rate, transmission power and medium access probability.

A. Medium Access in the Terrestrial Channel

Let us consider a network with M nodes. We assume that all nodes have independent S-N and N-N channels. We further assume that channel statistics are the same for all terminals, which is the case if the distances from node N_i to node N_j change little $\forall i, j \in \{1, \ldots, M\}$, $i \neq j$ and with respect to each node's distance to the source.

In our setup the terminals are set in *promiscuous mode* so that each node can receive the broadcast transmissions of any other node within communication range [29]. The terminals share the wireless medium, i.e., they transmit in the same frequency band. We assume that a CSMA/CA protocol is adopted by the nodes and that all nodes hear each other, so that the medium is shared among the terminals willing to transmit but no collision happens.

The communication rate z_{iJT} has been derived in [19] and has the following expression:

$$z_{iJT} = \frac{1 - (1 - p_a)^M}{M} \left[1 - (P_{NN})^{|T|} \right],\tag{11}$$

where $|T|$ is the cardinality of T, and the term $\left[1 - (P_{NN})^{|T|} \right]$ is the probability that at least one of the $|T|$ nodes whose S-link belongs to the cut receives correctly a transmission from a node that is in the other side of the cut. We do not report here the derivation for a matter of space. Note that Eqn. (11) is the rate at which packet are received by the set T considered as a single node, that is, the counting process $A_{iJT}(\tau)$ increases of one unit when at least one of the terminals in T receives one packet, independently from how many terminals receive it.

B. Coverage Analysis

In the following we derive the conditions that maximize the coverage as a function of relevant network parameters by applying the Max-flow Min-cut theorem. We recall that such maximum coverage can be attained by using the random coding scheme described in Section II.

Let us consider Eqn. (8). For each of the M nodes we must consider all the possible cuts of the network such that the considered node and the satellite are on different sides of the cut. Let us fix a receiving node N_t. We recall that a cut is a set of edges that, if removed from a graph,

separates the source from the destination. Fig. 2 gives an example of a network with four nodes where the cut Q_{SN_4} (i.e., the cut such that N_4 and S are on the same side) is put into evidence. In the example, the destination node is $N_t = N_1$. The dashed black lines represent the edges which are to be removed to get the cut. Note that the set of nodes that receive from S (only node N_4 in the figure) are isolated by the cut from the nodes with satellite cut (nodes N_1, N_2 and N_3 in Fig. 2). We define an *S-edge* as an edge of the kind $(S, N_j), j \neq t$. We further define a *T-edge* as one of the kind: $(N_j, N_t), j \neq t$. Unlike in [19], here each S-edge incorporates the effect of the availability of two different paths for the signal transmitted by S through S_1 and S_2 and the fact that the signals are combined at the physical level. This is reflected by the lower packet loss rate within each generation which is given by Eqn. (2). As mentioned in Section II this does not change the equivalent graph representation of the network. Hence the derivation of the coverage carried out in [19] is still valid, although only formally. Thus the expression of the coverage is given by equation (12) [19], where $Y_j = P_{SNj}$ is a r.v. representing the packet
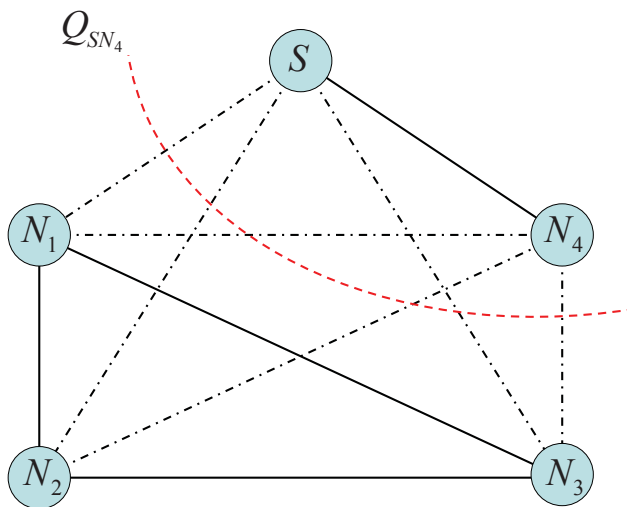

Fig. 2. Graph model for a network with four terminals. There are $2^{M-1} = 8$ possible cuts for each of the M nodes. The set of nodes that receive from S (only node N_4 in the figure) are isolated by the cut from the nodes with satellite cut.

loss rate within a generation for node N_j, Q_{n_s} is one of the cuts with n_s satellite links relative to the node N_t,

$$\alpha(n_s) = 1 - R + (M - n_s)\frac{1 - (1 - p_a)^M}{M}\left[1 - (P_{NN})^{n_s}\right], \tag{13}$$

while $\mathcal{S}(n_s, \overline{N}_t)$ is the set of subsets of $\mathcal{N} \backslash N_t$ with n_s elements. Although formally equivalent, Eqn. (12) differs from that in [19] in the Y variables, that in this case are given by Eqn. (2).

C. Lower Bound on Achievable Coverage

Although Eqn. (12) might be used to evaluate Ω numerically, a closed-form expression would give more insight into the impact of cooperation on the considered setup. Finding a simple closed form expression for Eqn. (12) is a challenging task. Thus in the following we derive a lower bound Ω_{LB} on Ω. Ω can be lower bounded by substituting in Eqn. (12) the packet loss rate Y_j for each cut with the largest packet loss rate among all the S-links in the network, i.e.:

$$
\Omega = Pr\left\{ \bigcap_{N_t \in \mathcal{N}} \bigcap_{n_s \in \{1,\ldots,M\}} \bigcap_{Q_{n_s} \in \mathcal{S}(n_s,\overline{N}_t)} \left[\prod_{j \in Q_{n_s}} Y_j < \alpha(n_s) \right] \right\}
$$

$$
\geq Pr\left\{ \bigcap_{N_t \in \mathcal{N}} \bigcap_{n_s \in \{1,\ldots,M\}} \left[\prod_{j=1}^{n_s} Y_{(j)} < \alpha(n_s) \right] \right\} \tag{14}
$$

$$
\geq Pr\left\{ \bigcap_{N_t \in \mathcal{N}} \bigcap_{n_s \in \{1,\ldots,M\}} \left[Y_{(1)}^{n_s} < \alpha(n_s) \right] \right\} \tag{15}
$$

$$
= Pr\left\{ \bigcap_{N_t \in \mathcal{N}} \bigcap_{n_s \in \{1,\ldots,M\}} \left[Y_{(1)} < \sqrt[n_s]{\alpha(n_s)} \right] \right\}
$$

$$
= Pr\left\{ Y_{(1)} < \min_{n_s \in \{1,\ldots,M\}} \sqrt[n_s]{\alpha(n_s)} \right\}
$$

$$
= \left(Pr\left\{ \frac{\Gamma_{S_1}}{\Gamma_{S_1} - \Gamma_{S_2}} e^{-\frac{2^r-1}{\Gamma_{S_1}}} - \frac{\Gamma_{S_2}}{\Gamma_{S_1} - \Gamma_{S_2}} e^{-\frac{2^r-1}{\Gamma_{S_2}}} > \beta \right\} \right)^M \tag{16}
$$

where $Y_{(i)}$ is the i-th largest packet loss rate across all S-edges of the network, i.e., $Y_{(i)} \geq Y_{(j)}$ if $i < j$, $\forall i, j \in \mathcal{N}$, and we defined

$$
\beta = \min_{n_s \in \{1,\ldots,M\}} \sqrt[n_s]{\alpha(n_s)}. \tag{17}
$$

$$
\Omega = Pr\left\{ \bigcap_{N_t \in \mathcal{N}} \bigcap_{n_s \in \{1,\ldots,M-1\}} \bigcap_{Q_{n_s} \in \mathcal{S}(n_s,\overline{N}_t)} \left[\prod_{j \in Q_{n_s}} Y_j < 1 - R + (M - n_s) \frac{1 - (1 - p_a)^M}{M} \left[1 - (P_{NN})^{n_s} \right] \right] \right\}.
$$

$$
\tag{12}
$$

Inequality (14) derives from the fact that:

$$\prod_{j \in S} Y_j \leq \prod_{j=1}^{n_s} Y_{(j)}, \text{ for } S \in \mathcal{S}(n_s, \overline{t}), \forall \; n_s, t, \tag{18}$$

i.e., we substitute the product of n_s random variables, chosen within a set of M variables, with the product of the n_s largest variables of the same set. Inequality (15) follows from the fact that

$$\prod_{j=1}^{n_s} Y_{(j)} \leq Y_{(1)}^{n_s}, \forall \; n_s, t. \tag{19}$$

Expression (14) can be further simplified in case one between the satellite link and the terrestrial link is strongly degraded. Using the result of Theorem 1 we find:

$$\lim_{\mu_j \to -\infty} \Omega_{LB} = \frac{1}{2^M} \left[1 - \text{erf} \left(\frac{10 \ln \left[\frac{1-2^r}{\ln(1-\beta)} \right] - \mu_i}{2\sigma_i^2} \right) \right]^M \tag{20}$$

where $j = 1$ or $j = 2$ if the degraded link is the one from the satellite or from the gap-filler, respectively.

V. COOPERATIVE COVERAGE EXTENSION IN DVB-SH

In the following we propose a practical scheme that implements the cooperative approach described in the previous section in heterogeneous satellite vehicular networks.

A. Space Segment

1) Satellite Channel: The considered setup is an LMS system with a GEO satellite in L band (or low S band) broadcasting a DVB-SH-B (time-division multiplexing (TDM) waveform from satellite and OFDM from the gap-fillers) signal to a population of mobile terminals. Propagation conditions change due mainly to the shadowing effect of building and trees and are classified in urban, suburban and rural. The main cause of channel impairment in urban and suburban environments is the long-lasting shadowing of the buildings that causes an intermittent satellite connectivity, while in the rural propagation scenarios the main source of impairment is tree shadowing. Signal reception in LMS systems is limited by three phenomena, namely path loss at large scale, shadowing at mid-scale and multipath fading at small scale. We adopt the Perez-Fontan (LMS) channel model [33], based on a three-state Markov chain in which the possible

states represent line of sight reception, moderate shadowing reception and deep shadowing reception. In each of the states the signal amplitude is modeled as a Loo process (sum of a Log-normal and a Rayleigh random variables) with different parameters.

2) Channel Impairment Countermeasures in DVB-SH: In this section we recall the channel impairment countermeasures foreseen in the DVB-SH standard.

a) Physical Layer: The physical layer error protection scheme of the DVB-SH standard are the duobinary turbo code, with different rates/word lengths, the bit interleaver, which works at bit level within a turbo codeword, and the time interleaver, the depth of which spans more than one codeword and uses interleaving blocks of 126 bits each. This last element is particularly important to counteract long blockage periods, as it can span time intervals of up to about 10 seconds. The drawbacks in using a long time interleaver are the large decoding delay and the memory requirements at mobile terminals, which can be met only by high class nodes.

b) MPE-IFEC in DVB-SH: The MPE-IFEC is a process section between the IP and the transport layers introduced in DVB-SH in order to counteract the disturbances in reception and transmission. This is achieved by applying a packet level FEC over multiple *datagram bursts*, i.e., groups of datagrams. The long high-layer interleaver used in IFEC allows for significant performance enhancements with respect to FEC [1], as it can better counteract long lasting shadowing which is typical of the LMS channel. The encoding is made over several datagram bursts. Let us consider a datagram burst entering the MPE-IFEC process. The burst is reshaped in a matrix of T by C bytes called Application Data Sub-Table (ADST). The columns of the ADST are then distributed in a round robin fashion among B matrices called Application Data Tables (ADT). An ADT is a T by K matrix. The FEC, always systematic, is applied on the ADT producing a T by N_r parity matrix, called IFEC Data Table (iFDT). An ADT is filled up and the encoding takes place every EP bursts, EP being the Encoding Period, which determines the number of datagram bursts over which the parity is calculated. The ADT and the iFDT together form an *encoding matrix*. It takes $B \times EP$ bursts to fill up a single ADT. Once an ADT is full (this happens to B ADT at the same time) the iFDT is calculated. As soon as the B iFDTs are calculated an *IFEC burst* is generated by taking groups of columns from S different iFDTs. An IFEC burst is made up of several IFEC sections. Each section is comprised of a header, a payload containing g columns from the same iFDT and a cyclic redundancy check (CRC). The k-th IFEC burst is merged with the $(k - D)$-th datagram burst (and eventual MPE-FEC

redundancy) to form a *time-slice burst*. The time slice burst is then multiplexed on MPEG2-TS frames and passed down to lower layers.

Depending on the FEC technique applied, different values of EP, B and S are adopted. In case a Raptor code is used EP is generally greater than 1, while $B = S = 1$. This is because Raptor codes, unlike other FEC codes such as Reed-Solomon codes [34], are capable of handling large source matrices (i.e., ADT), that can span several datagram bursts.

The Raptor code adopted for the DVB-SH is the same as in the 3GPP standard, which has also been adopted in the DVB-Handheld (DVB-H) standard [1]. Its description can be found in [35]. A source block in [35] corresponds to an ADT and a source symbol is a column of the ADT. Thus a source block has K symbols of T bytes each. The Raptor encoder is applied independently to each source block, each of which is identified by a Source Block Number (SBN). The encoder produces K systematic symbols (the ADT matrix) and N_r *repair* (parity) symbols. In Fig.3 the ADT matrix is shown (on the left) together with the parity matrix (on the right). The reshaped datagrams composing the ADT are also shown for sake of clarity.
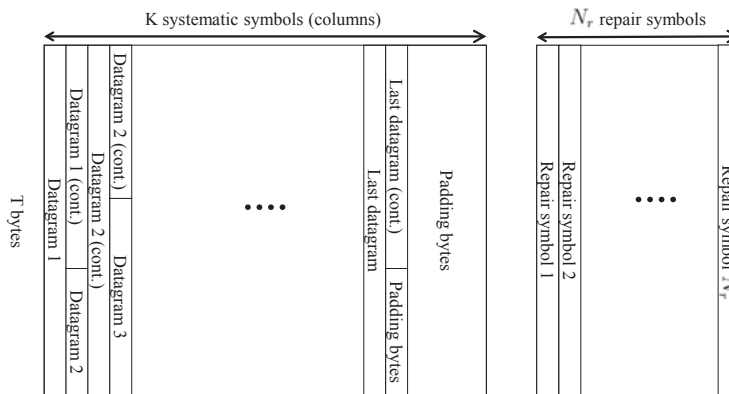

Fig. 3. Reshaping of datagram bursts in an ADT (left) and parity matrix (right) in case a Raptor code is used.

Systematic and repair symbols are called *encoding symbols*. Each symbol is identified by an Encoding Symbol Identifier (ESI). Values from 0 to $K - 1$ are assigned to the systematic symbols, while values from K to $N_r + K - 1$ identify repair symbols. The encoding procedure consists of two parts. In the first part L *intermediate symbols* are produced starting from the K source symbols, while in the second part $K + N_r$ encoding symbols are generated starting from

the L intermediate symbols.

The intermediate symbols from 0 to $K-1$ are systematic (i.e., are the source symbols). The S intermediate symbols from K to $K+S-1$ are generated using an LDPC encoder while the last H symbols from $K+S$ to L are called *Half Symbols* and are generated using a binary reflected Gray encoder [1].

The encoding symbols are generated applying a Luby Transform (LT) encoder to the L intermediate symbols. The LT encoder operates a bit-wise XOR of intermediate symbols chosen according to a certain degree distribution. Each of the encoding symbols is transmitted together with its ESI and a triple (d, a, b) where d is the symbol degree and a and b are integers from the sets $1, \ldots, L'' - 1$ and $0, \ldots, L'' - 1$ respectively, $L'' - 1$ being the smallest prime integer greater than or equal to L. At the end of the encoding process, K systematic symbols plus N_r parity symbols are produced. The parity symbols are linear combinations of systematic symbols in $GF(2)$. The encoding symbol triple together with the ESI and the value K allows the decoder to determine which intermediate symbols (and thus which source symbols) were combined to form each of the encoding symbols.

B. Ground Segment

1) Terminal Types: We consider high class terminals as defined in [23]. High class terminals are not energy constrained and have relatively good computation capabilities and memory [23]. This is the case of vehicular terminals, which are powered by rechargeable batteries and can host computation units of high speed, thanks to the relative low impact in terms of cost, space and weight. We assume that each terminal has both satellite and short-range communication capabilities, which give rise to the possibility of implementing a vehicular capillary network.

2) Terrestrial Channel: A possible classification of the VtoV communication channel is based on roadside environments such as buildings, trees and bridges. In this case the propagation scenarios are categorized as urban canyon, suburban street and expressway. Signal propagation in VtoV systems has been studied in [36], [37] and [38].

In [39] a measurements campaign made on the 5.9 GHz frequency is presented. The measurements presented in [39] have been made using a Dedicated Short Range Communication (DSRC)/IEEE 802.11p prototype radio. In the paper a dual slope model for the path loss in urban VtoV scenarios is derived based on real measurements. We adopt the model of [39] for

the path loss together with the TU6 multi-tap channel model [40]. An OFDM signal with 52 carriers (48 information carriers) and a rate $1/2$ convolutional encoder are assumed. All physical layer parameters are taken from the 802.11p standard. As usual practice in VtoV simulations, we assume a finite communication range which is fixed for all vehicles. Furthermore, we take into account collisions as they constitute an important throughput-limiting and delay-increasing factors in ad-hoc wireless networks [41].

VI. NETWORK-CODED COOPERATION FOR DVB-SH

The analysis carried out in Section IV gives hints about the advantages and the limits of cooperation in providing missing coverage in mobile satellite networks. Although useful to understand the effect of relevant system parameters such as the number of nodes, the probability of accessing the terrestrial channel and the physical layer channel statistics, many other interacting factors are present in a real system, that can not be accurately taken into account in a mathematical way without incurring in a model which is overwhelmingly complex. Among these factors are the specific communication standard involved in the system, that may show a gap with respect to the theoretical performance derived in Section III and IV. What actually makes the difference is not the performance of the physical layers *per se*, since in DVB-SH highly efficient codes are adopted that can get close to the information theoretical bounds, but the interaction between the physical layer of the standard and the propagation channel, that can have complex and unpredictable behaviors. Such interaction determines certain packet loss patterns at the higher layers, where the throughput of the system is measured. Apart from this, the changing terrestrial network topology and connectivity together with the imperfections in the medium access mechanism further complicate the picture. A possible implementation of the cooperative approach described in the previous sections has been presented in [20]. Such scheme has been designed in order to be able to live together with existing communication standards without the need of modifying them. The main novelty with respect to [20] is the enhancement in the MATLAB/C++ - based simulator used to evaluate the performance of the NCCCE protocol. The main differences are the inclusion of a gap-filler, the implementation of the physical layer of 802.11p standard (modulation, channel code and a simplified version of the channel access mechanism), the use of widely adopted channel models to generate the time series in the terrestrial channels (both vehicle-to-vehicle and gap-filler-to-vehicle) and two key

features of the DVB-SH-B standard, namely the physical layer combining of the signals received from the satellite and the CGC at the terminal nodes and the DVB-SH Raptor encoder. All these features were not taken into account in the preliminary simulation results presented in [20]. In the following we present the proposed cooperation protocol named Network-Coded Cooperative Coverage Extension (NCCCE).

Let us consider a satellite broadcasting a DVB-SH-B signal with MPE-IFEC protection to a population of vehicular terminals with both DVB-SH-B and IEEE 802.11p radio interfaces. During a time window $(0, t)$ the satellite transmits $K + N_r$ IFEC symbols obtained from an ADT. Terrestrial and satellite communications take place in orthogonal frequency bands. Due to long-lasting shadowing caused by urban propagation conditions, it can happen that a user decodes a number of symbols equal to $M < K$ during the interval $(0, t)$. In this case the user cannot decode the entire source data block. In order to enhance satellite coverage each node re-encodes the received packets (either received directly from the satellite or from other terminals) and broadcasts them to nodes within its transmission range. In Fig. 4 a block diagram of the proposed cooperative method is shown. In the following sections we describe the encoding
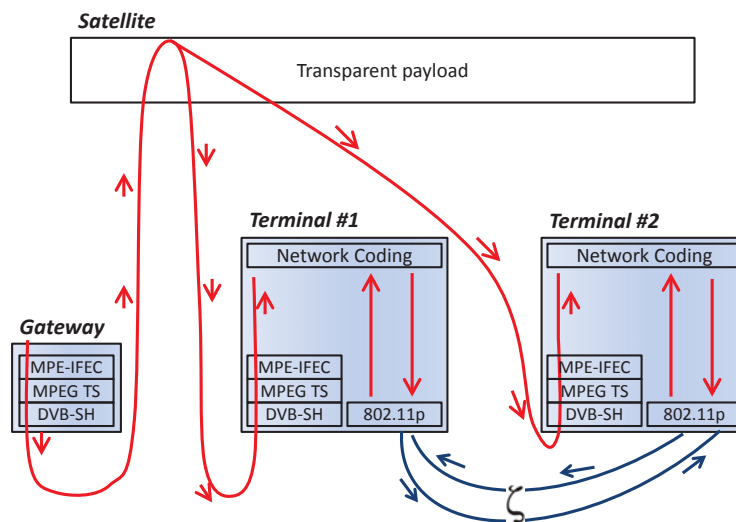

Fig. 4. Block diagram of the proposed cooperative scheme for two cooperating nodes. Red lines represent IFEC blocks flowing from the satellite to the terminal nodes while blue lines represent network coded packets exchanged between nodes on the short range communication channel.

procedure at land mobile nodes.

A. Encoding at Land Mobile Nodes

Let us assume that a node is able to decode some of the encoding symbols directly from the satellite. Each symbol carries an ESI and a triple (d, a, b). As described in Section V-A2b the node can use this information to find out which of the source symbols were combined together to form that encoding symbol. We propose to apply a network encoding scheme at land mobile nodes using the source symbols of iFEC as source symbols of the network code. In other words, nodes exchange linear combinations of encoding symbols in some finite field, with the aim of recovering all the source symbols.

B. Terrestrial Channel Usage

Each received encoding symbol is interpreted by a node as a linear combination of source symbols with coefficients 0 or 1 in $GF(q)$. The node, then, applies the network encoding procedure described in Section II. The encoding vector of the received encoding symbol can be derived from symbol's ESI and triple (d, a, b).

The probability to access the channel in each slot is determined by the parameter *cooperation level*, fixed for all nodes, which we indicate with ζ, $0 \leq \zeta \leq 2$. If $\zeta \leq 1$, in each slot, if a node stored a number of linearly independent packets which is larger than the number of transmitted packets in the current generation, it creates a linear combination of all the stored packets as described in Section IV and tries to access the channel with probability ζ. If $\zeta > 1$ two cases must be considered. In case the number of transmissions made by the node is lower than the number of linearly independent packets received, the node tries to access the channel with probability $p_a = 1$. If the node has a number of stored packets which is lower than or equal to the number of those transmitted, instead, it tries to access the channel with probability $p_a = \zeta - 1$.

When a node receives a packet from another node, it checks whether the packet is linearly independent with the stored packets and, if this is the case, the new packet is stored. If the received packet is not linearly independent with the stored ones, it is discarded.

Another possible relaying choice is to have the nodes simply forwarding the received symbols without combining them. We call this scheme *simple relaying* (SR) and use it as a benchmark. SR is described more in detail in Section VIII.

C. Implementation Aspects

According to the DVB-SH standard we consider a source symbol size of 1024 Bytes each. Each source symbol is divided into n_{ss} subsymbols, each of which containing $\frac{1024}{n_{ss}}$ bytes. Each of these subsymbols is multiplied by a randomly chosen coefficient in a field with $q = \frac{1024}{n_{ss}} 2^3$ elements. The coefficient is the same for all subsymbols within a symbol. In this way the complexity of the network encoder/decoder can be kept at a reasonable level [12]. A field size of 2^8 or 2^{16} (one or two bytes) may constitute a valid choice. The NC is applied as in [12], adding the encoding vector at the end of each packet. Thus, for a K symbols generation, a header with $K \times q$ bits is appended to each symbol. The loss in spectral efficiency is then $(Kq)/8192$. Assuming coefficients of 1 byte are used, the loss becomes $K/1024$. In order to keep the loss at a reasonable value we should limit the size of the generation. For instance, if generations of $K = 100$ symbols are used, the loss is below 10%. The adoption of small generation sizes has the drawback that the code efficiency is reduced. For example, it is known that the efficiency of the Raptor code increases with the source block. There is, however, advantages in using small blocks. Actually, if a short interleaver is used together with blocks of small size, the data is readily available to the upper layer sooner than in the case of large blocks, i.e., the delay decreases. In Section IX we show the gap between the asymptotic results obtained in Section IV and the simulation results obtained in the same setup but with the 3GPP Raptor code, having finite block-length.

VII. Interaction of Physical Layer and Upper Layers

In order to evaluate numerically the performance of the proposed methods at system level, the simulator must be capable of taking into account the channel impairments of the physical layer. In order to do this, physical layer simulations should be run for each of the nodes, taking into account the channel characteristics and the error correction capabilities of the considered PHY layer standard as done in [42]. Such approach is, however, extremely time consuming, which makes it unfit for a system level simulation. A valid alternative is given by the PLA [24] [25] The use of PLA allows to take into account the effects of physical layer elements such as coding, modulation and the presence of an interleaver, at system level in a computationally manageable way. This is particularly useful in case of time-selective channels, in which the channel gain changes within the duration of a codeword. The PLA has been widely studied in the last decade

achieving a growing accuracy for a wide range of transmission setups. A method used in the past to obtain instantaneous link performances is the average signal to interference plus noise ratio (SINR) mapping, which consists in calculating the arithmetic (or geometric) average SINR experienced by the channel symbols of a codeword and map such average on the FER curve in AWGN for the considered code and modulation. This technique shows in general an optimistic behavior of the channel, as high SINR experienced in some parts of the codeword would distort the results.

In more recent types of PLA the instantaneous symbol SINR vector is compressed in a single SINR value, the effective SINR ($SINR_{eff}$). Such approach is called *effective SINR mapping* (ESM). Several ESM PHY abstraction methods have been proposed in the literature based on mean instantaneous capacity, exponential-effective SINR mapping and Mutual Information Effective SINR Mapping (MIESM). A more detailed description as well as more references for these methods can be found in [26]. The $SINR_{eff}$ in the ESM methods is obtained as follows:

$$SINR_{eff} = \Phi^{-1} \left(\frac{1}{n} \sum_{i=1}^{n} \Phi(SINR_i) \right), \tag{21}$$

where $\Phi(x)$ is an invertible function that depends on the specific ESM method and n is the codeword length. In MIESM such function can be related to the mutual information per received coded bit. This approach is referred to as RBIR. The function $\Phi(x)$ is provided by the so called *modulation-channel model* through a function obtained by normalizing the modulation-constrained symbol mutual information (SI) vs SNR function. Once $SINR_{eff}$ is obtained, it is used to determine the FER using curves for the considered channel code in AWGN. Note that $SINR_{eff}$ is referred to the coded symbol, which means that modulation order and coding rate must be taken into account before using it in the FER curves. If, for instance, E_b/N_o FER curves are used, the $SINR_{eff}$ must be multiplied by a factor $\frac{1}{\log_2(M_o)r}$, M_o and r being the modulation order and the coding rate, respectively.

We implemented a simulator that uses the RBIR approach and validated it by comparing the obtained FER curve with that resulting from the simulation of the whole transmission chain. The results of the RBIR validation are not reported here for a matter of space but can be found in [20].

VIII. SIMULATION SETUP

We evaluated the performance of the proposed scheme by developing a simulator that models a satellite to land mobile broadcast transmission over DVB-SH-B. 150 nodes were randomly placed on a Manhattan grid of one square kilometer with 10 intersecting roads. The distance between two parallel roads is 110 m. Each node moves at a speed of 50 km/h along one of the roads, keeping a constant direction of motion during the whole simulation. The direction of motion is chosen at random for each node. When a node reaches the border of the map it enters back into the map from the opposite side, as is common practice in this kind of simulations. Nodes can communicate with each other and have network coding capabilities. Communication can take place between two nodes only if they are within a radius of 300 m. A combination of the path loss model derived in [39] and the TU6 multi-tap propagation model is used. The coding and modulation considered are the ones of 802.11p, namely OFDM modulation and rate $1/2$ convolutional code at 5.9 GHz. The correctness of the reception is evaluated through PLA. One IFEC block of $K = 150$ IFEC symbols is transmitted at each trial. In the following we will use interchangeably the terms "IFEC block" and "generation". Each block contains K source symbols of 1024 bytes each. The total number of coded symbols transmitted for a single generation is $\lceil K/R_{IFEC} \rceil$, where R_{IFEC} is the rate of the Raptor encoder and $\lceil x \rceil$ is the smallest integer larger than or equal to x. We use the 3GPP Raptor encoder described in [35]. Each IFEC symbol is encapsulated within an MPEG2 TS packet and sent to the channel encoder. The channel encoder is the 3GPP2 turbo encoder specified in [43]. Each source message of the channel encoder has a fixed length of 12288 bits, which means that about one and a half IFEC symbols fit within one Turbo codeword. Once encoded with a rate R_{turbo} the IFEC symbols are first interleaved with the bit interleaver and successively with the time interleaver, which provides time diversity to the signal. In the simulator we implemented two of the time interleavers described in [23], namely the *short uniform* interleaver and the *long uniform* interleaver. The former has a depth on the order of 200 milliseconds while the latter has a depth on the order of 10 seconds. After time interleaving, the bits are QPSK modulated and transmitted with a roll off factor equal to 0.35. For each of the mobile nodes we generate a channel series using a generator implementing the three state Perez-Fontan LMS channel model. The correctness of the reception of each turbo codeword is evaluated using PLA as described in Section VII, taking into account data rate,

channel interleaver, channel code rate, and other relevant parameters. In the setup in which the gap-filler is present, an OFDM modulation with 6048 carriers and a guard interval GI of 224 microseconds is used by the gap-filler. All parameters conform to the DVB-SH-B standard. The propagation model from the gap-filler to each of the nodes is a combination of the modified COST 231 Hata path loss model with the classical TU6 channel model, as suggested in [1]. The signals from the satellite and the gap-filler are combined at the physical level by the receiver using maximal-ratio combining. The same channel code and interleaver are used in both the satellite and the gap-filler. The gap-filler is located at a distance $d_{gap\_fill} < GI \cdot c$ from the center of the map, where $c = 3 \cdot 10^8$ m/sec is the speed of light. The link budget adopted for the satellite network is the one in [1], Table 11.28. The table I below summarizes the main simulation parameters. Depending on the sequence of correctly decoded codewords, the decoded IFEC symbols can be determined. Nodes exchange IFEC messages using DSRC/IEEE 802.11p interfaces. The transmission rate in the ground segment is set high enough so that an IFEC symbol can be transmitted before the next one is received on the satellite channel. The MAC mechanism in the terrestrial segment is CSMA as in 802.11p. Nodes are set in *promiscuous mode* so that each node can receive the transmissions of any other node.

We compare two different relay methods. One is the NCCCE scheme described in Section VI, which is based on network coding. The other relay scheme is the simple relaying (SR) scheme, also introduced in Section VI. Unlike in the NCCCE scheme, in SR nodes do not combine IFEC symbols, they just transmit the oldest non transmitted packet. In SR, if all the received packets have already been transmitted, then, if $\zeta > 1$, a node transmits (with probability $1 - \zeta$) a randomly chosen packet.

The amount of received data is measured at the interface between the IFEC and the upper layers, as indicated in Fig. 5, considering the IFEC block as a fundamental data unit. The reason for this choice is that data coming from the upper layers are reshaped in the ADST's. Thus, receiving one or more IFEC symbols, even if systematic, may not be useful, as they are part of a larger bunch of data like, e.g., firmware or road map updates, or may be parts of incomplete IP datagrams. Thus when we refer to *decoded data* we mean decoded IFEC blocks. The decoding is possible if and only if a number of linearly independent IFEC coded symbols equal to the number of IFEC source symbols is correctly received. The decoding is possible since each of the IFEC coded symbols, as well as each of the NC packets, embeds information about which

TABLE I

SIMULATION PARAMETERS.

Environment	Urban
Satellite carrier frequency	2.2 GHz
Satellite SNR (LOS)	12 dB
Time interleaver depth	200 ms - 10 s
Modulation	QPSK
Roll-off factor	0.35
Bandwidth	5 MHz
LL-FEC symbol size	1024 bytes
Size of LL-FEC blok (K)	150 ($\sim$ 150 kB)
Rate Turbo Code	1/2
Rate Raptor Code	1/4
Gap-filler distance (d_{gap_fill})	3 km
Gap-filler carrier frequency	2.12 GHz
EIRP gap-filler	25 dBW
Number of gap-filler OFDM carriers	6048
Subcarrier spacing gap-filler	0.69754 kHz
Scenario surface	1 sq. km
Number of terminals	150
Terminal type	Vehicular
Terminal speed	50 km/h
V2V carrier frequency	5.9 GHz
V2V transmission power	20 dBm
Number of IEEE 802.11p OFDM carriers	52
Subcarrier spacing IEEE 802.11p	0.15625 MHz
Conv. code rate IEEE 802.11p	1/2

source symbols were combined to form it, and thus common matrix manipulation techniques can be used to retrieve the source symbols.

IX. NUMERICAL RESULTS

Fig. 6 shows the coverage Ω, obtained by evaluating numerically Eqn. (12), plotted against the rate at physical level r for a fixed message rate R and different network sizes. The relative lower bounds and the coverage curve in case of no cooperation are also shown. In the simulation

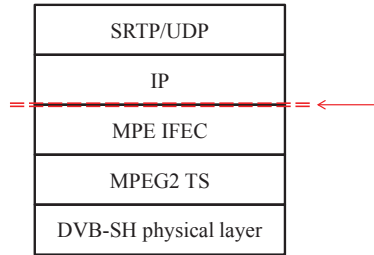| SRTP/UDP |
|---|
| IP |
| MPE IFEC |
| MPEG2 TS |
| DVB-SH physical layer |

Fig. 5. The amount of received data is measured at the interface between the IFEC and the upper layers.

we assumed that one between the satellite and the gap-filler links is affected by severe fading and set $R = 2/3$, $p_a = 0.2$, $\Gamma_N = 10$ dB in the N-N channel, $\mu = 3$ and $\sigma = 1$ in the S-N channel for the available link. It is interesting to note how increasing the number of nodes also increases the achievable rate r for a given Ω. This is because the higher is the number of nodes, the higher is the probability that all the information broadcasted by S reaches at least one node of the network, i.e., it has not been lost. Once the information has reached the network, it can be efficiently distributed among the terminals using RLNC. An important gain in the transmission rate can be observed, with an increase of about 0.4 bpcu when passing from no cooperation to cooperation in a network with 2 nodes, and about 1 bpcu in case of a network with 4 nodes. The lower bound is fairly tight for $M = 2$ and $M = 4$. We point out that this result is achieved without any feedback to the source or any packet request among nodes, as the decision on whether to encode and transmit or not is taken autonomously by each terminal depending on the probability of media contention p_a. As mentioned in the previous sections such performance curves are *achievable*, which implies infinite code lengths must be used. In order to evaluate the loss in performance due to finite code lengths and real coding schemes implementation, we also show in Fig. 6 the curves obtained for the same setup but with a finite block-length Raptor code. The Raptor encoder is the one used in DVB-SH and introduced in Section VIII[3]. A block length of $K = 150$ source symbols was chosen. We see that, although an important gain in terms of physical layer rate is achieved thanks to cooperation and such gain increases

---

[3]Note that, although in principle a Raptor decoder is meant to be decodable through iterative cancellation, in DVB-SH, as well as in other practical standards, the iterative algorithm is only the first decoding step, since, in case of blocking, Gaussian elimination is applied. This decoding process has been implemented in our simulator.

with the number of terminals as in the asymptotic case, a gap between theoretical and numerical results is present. This is due to the finite and relatively small block length. Such gap can be reduced by applying NC directly in the space segment [44]. However, such approach has the drawback that the decoder complexity is higher also in case no cooperation is used, which is not the case when a Raptor code is adopted. Moreover, it would imply a modification in the satellite segment, which, in our proposed scheme, remains unaltered. In Fig. 7 the coverage is plotted
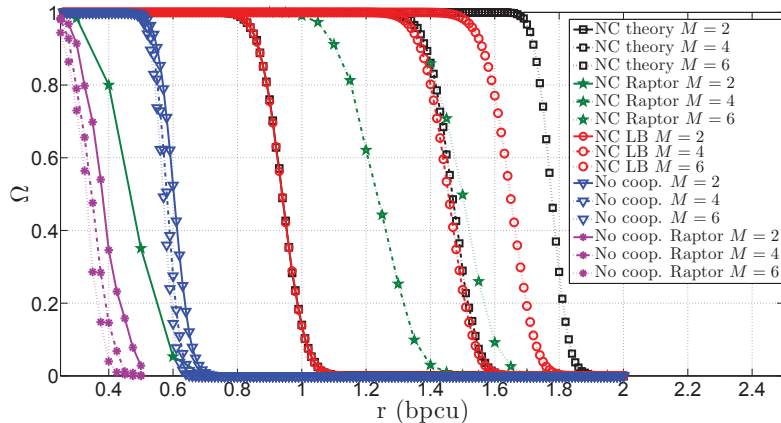

Fig. 6. Coverage Ω plotted against rate at physical layer r in the cooperative case for different values of M. The lower bound and the non cooperative case are also shown. In the simulation we set $R = 2/3$ messages/slot, $p_a = 0.2$, $\Gamma_N = 10$ dB in the N-N channels, $\mu = 3$ and $\sigma = 1$ in the S-N channel.

against the per-node probability of transmission attempt p_a for $M = 4$, $\Gamma_N = 10$ dB, $r = 1$ bpcu and $R = 2/3$. It is interesting to note that relatively small values of p_a (lower than 0.15 for the asymptotic case) are sufficient to achieve full coverage for values of r and R which are of practical interest. We further observe that the lower bound tightly approximates the simulated theoretical curve. In the figure we also plotted the curve for the case of a practical cooperative scheme using the 3GPP Raptor code with source block length $K = 150$. As in Fig. 6, the loss with respect to the theoretical curve is due to the finite block length. The coverage for the non cooperative case in the setup considered in Fig. 7 is 0, coherently with Fig. 6.

In the rest of the section we compare the performance of the three practical schemes described in previous sections. One is the NCCCE system described in Section VI, one is the SR system described in Section VIII while the last system we consider is a non cooperative system in which the nodes can receive only from the satellite (or from the satellite + gap-filler, when
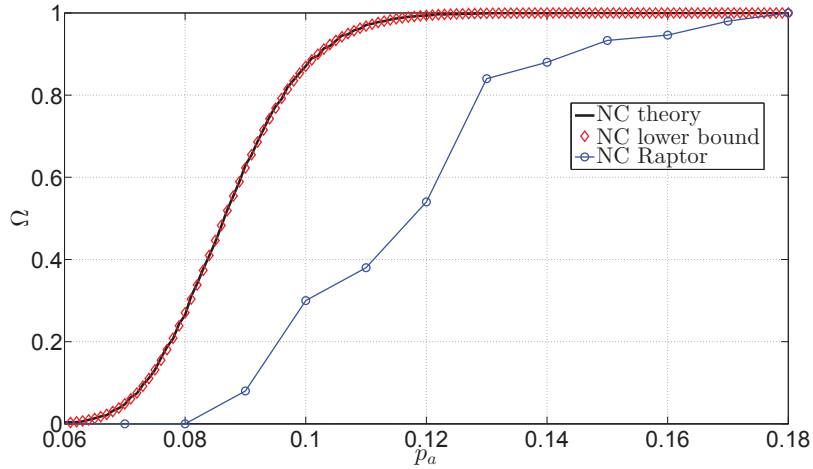
Fig. 7. Coverage Ω plotted against the probability of media contention p_a in the cooperative case for a network with $M = 4$ and $\Gamma_N = 10$ dB. The lower bound Ω_{LB} curve and the curve of a practical scheme with finite block length Raptor code are also shown. In the simulation we set $R = 2/3$ messages/slot, $r = 1$ bpcu, $\mu = 3$ and $\sigma = 1$ in the S-N channel.

considered). We consider as performance metric the average percentage of nodes that receive all the transmitted data. The metric is evaluated for different values of the cooperation level ζ in the range $[0, 2]$. Note that the system with satellite only reception corresponds to a cooperative system with $\zeta = 0$. Considering different values of ζ we can evaluate the performance gain of the cooperative methods with respect to the non cooperative system as a function of the terrestrial channel utilization. Fig. 8 shows the average percentage of nodes that receive all data plotted against ζ. In the simulations we set the rate at physical level to $1/2$ while the rate of the Raptor encoder has been set to $R_{IFEC} = 1/4$. The short interleaver has been used. We also evaluated the case of long interleaver with and without gap-filler and with no IFEC protection (which corresponds to a Raptor rate of $R_{IFEC} = 1$). We did not consider the case of long interleaver with forward error correction because, according in the DVB-SH-B standard, the IFEC protection is meant to be applied only in combination with the short interleaver. In case the long interleaver is used together with a gap-filler (not shown in the figure) 100% of the nodes are covered. The NCCCE scheme achieves the best performance among all others setups, with a gain of about 25% with respect to the non cooperative scheme and a gain of about 29% with respect to the SR scheme in case no gap-fillers are user (w.o. gf). A notable fact that emerges
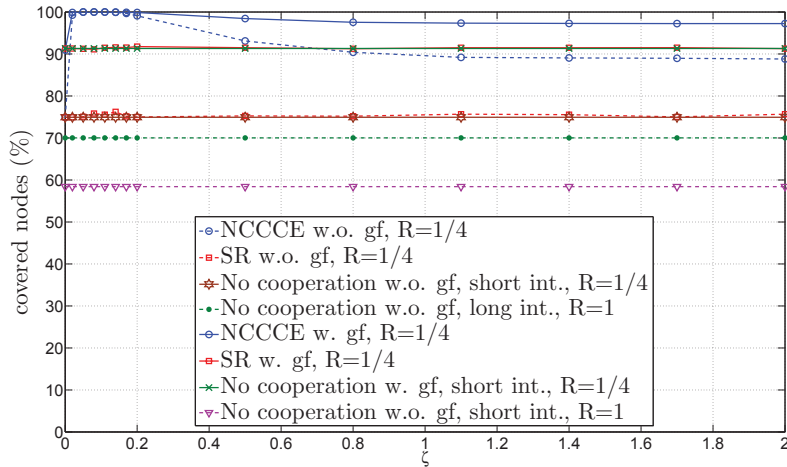
Fig. 8. Average percentage of nodes that decode all data plotted against the cooperation level ζ for NCCCE, SR and the non cooperative scheme. The rate couple $(r, R) = (1/2, 1/4)$ has been set in the simulation and the DVB-SH short interleaver has been considered. The non cooperative case with long interleaver and $R = 1$ is also shown for comparison.

from the plots is that full coverage is achieved by the NCCCE scheme with little use of the terrestrial channel for $\zeta = 0.05$ either in case a gap-filler is used or not. The performance of the scheme worsens as ζ approaches 2. This is due to the fact that the terrestrial channel load increases with ζ, determining an increase in the number of collisions and thus diminishing the spectral efficiency of the capillary network. We further notice that this is similar to what shown in Fig. 7, in that the maximum advantage of the network-coded cooperative scheme is achieved for small values (smaller than 0.15) of the channel access probability p_a. From Fig. 8 we also notice that the NCCCE scheme with short interleaver achieves a higher percentage of covered nodes with respect to the non cooperative configuration with long interleaver. On the one hand this result suggests that a short interleaver can be used instead of a long one, with a huge memory saving in the physical layer architecture of the receiver. Of course this comes at the expense of larger memory resources at higher levels (IFEC), which are likely to have, however, an overall cost which is lower than the memory at lower levels. On the other hand, for a fair comparison we must take into account that the long interleaver scheme does not use IFEC protection, which implies a gain in terms of spectral efficiency of $1/R_{IFEC} = 4$, i.e., there is a tradeoff between complexity and transmission rate.
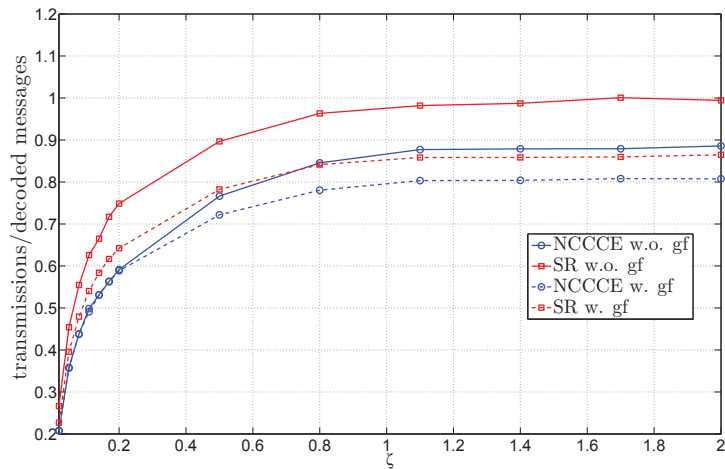
Fig. 9. Average number of transmissions needed to decode one IFEC symbol plotted against the cooperation level for the NCCCE and the SR schemes. The NCCCE scheme makes a much more efficient use of terrestrial channel resources.

The gain in terms of percentage of covered nodes of the cooperative schemes with respect to the non cooperative case derives from the use of the terrestrial channel bandwidth. In order to evaluate which between the NCCCE scheme and SR scheme uses such resources more efficiently, we plot the average number of retransmissions needed to decode a message (IFEC symbol) against ζ in Fig. 9. From the figure we see how the NCCCE needs on average less transmissions per decoded message with respect to the SR scheme in the whole range of ζ considered. From Fig. 8 and Fig. 9 emerges that the NCCCE scheme achieves a larger gain in terms of percentage of covered nodes with respect to the SR scheme using the resources of the terrestrial channel in a more efficient way.

X. CONCLUSIONS

We investigated the performance of a cooperative approach in providing missing coverage for heterogeneous LMS networks in the presence of both a direct satellite link and a link from a terrestrial repeater. We carried out an analytical study considering a mathematically tractable and yet practically interesting network model assuming a combination of the signals from the two links if performed by the receivers at the physical level. Fading and shadowing effects in both links as well as the medium access mechanism in the V2V network have been taken into

account. By applying the Max-flow Min-cut theorem we derived an exact expression for the coverage as a function of both the information rate at physical layer and the rate of innovative packets injected in the network per unit-time as well as a closed form expression of a lower bound in case one of the two physical links is severely degraded. Our results give a tradeoff between the coverage and the rate at which the information can be injected in the network, and at the same time quantify the gain derived from node cooperation through the short range interface. We showed that the diversity gain grows with the number of terminals, opening up the possibility of increasing the transmission rate at the source source while still guaranteeing a good coverage.

Based on the considered theoretical model we proposed a practical cooperative scheme which leverages on network coding for enhancing coverage in heterogeneous satellite vehicular LMS systems over DVB-SH, which does not require any modifications at the lower layers. Our numerical results, based on physical layer abstraction, showed that a cooperative relaying system based on random linear network coding can bring important benefits in terms of both coverage and terminal complexity with respect to a system in which nodes receive from satellite only, as well as with respect to a relaying scheme in which network coding is not used. As a final remark we point out that the delay induced by the NC decoding as well as the relative memory requirements are essentially the same in the proposed scheme an in DVB-SH LL-FEC, since the NC encoding is done only within an LL-FEC block. This is because the terminals need to buffer only network coded packets relative to the same LL-FEC block, which would also be the case if LL-FEC was applied without NC.

APPENDIX

Proof of Theorem 1

$$Pr\left\{\frac{\Gamma_{S_j}}{\Gamma_{S_j}-\Gamma_{S_i}}e^{-\frac{2^r-1}{\Gamma_{S_j}}} - \frac{\Gamma_{S_i}}{\Gamma_{S_j}-\Gamma_{S_i}}e^{-\frac{2^r-1}{\Gamma_{S_i}}} > R\right\} = Pr\left\{\frac{\Gamma_{S_j}}{\Gamma_{S_j}-\Gamma_{S_i}}\left(e^{-\frac{2^r-1}{\Gamma_{S_j}}} - e^{-\frac{2^r-1}{\Gamma_{S_i}}}\right) + e^{-\frac{2^r-1}{\Gamma_{S_i}}} > R\right\}$$

$$= Pr\left\{\frac{\Gamma_{S_j}}{\Gamma_{S_j}-\Gamma_{S_i}}\left(e^{-\frac{2^r-1}{\Gamma_{S_j}}} - e^{-\frac{2^r-1}{\Gamma_{S_i}}}\right) + e^{-\frac{2^r-1}{\Gamma_{S_i}}} > R \,\middle|\, e^{-\frac{2^r-1}{\Gamma_{S_i}}} > R\right\} Pr\left\{e^{-\frac{2^r-1}{\Gamma_{S_i}}} > R\right\}$$

$$+ Pr\left\{\frac{\Gamma_{S_j}}{\Gamma_{S_j}-\Gamma_{S_i}}\left(e^{-\frac{2^r-1}{\Gamma_{S_j}}} - e^{-\frac{2^r-1}{\Gamma_{S_i}}}\right) + e^{-\frac{2^r-1}{\Gamma_{S_i}}} > R \,\middle|\, e^{-\frac{2^r-1}{\Gamma_{S_i}}} \leq R\right\} Pr\left\{e^{-\frac{2^r-1}{\Gamma_{S_i}}} \leq R\right\}$$

$$\text{(22)}$$

The first term of the sum in Eqn. (22) can be written as:

$$Pr\left\{\frac{\Gamma_{S_j}}{\Gamma_{S_j}-\Gamma_{S_i}}\left(e^{-\frac{2^r-1}{\Gamma_{S_j}}}-e^{-\frac{2^r-1}{\Gamma_{S_i}}}\right) > R-e^{-\frac{2^r-1}{\Gamma_{S_i}}} \mid R-e^{-\frac{2^r-1}{\Gamma_{S_i}}} < 0\right\} Pr\left\{e^{-\frac{2^r-1}{\Gamma_{S_i}}} > R\right\}$$

$$= Pr\left\{e^{-\frac{2^r-1}{\Gamma_{S_i}}} > R\right\}, \quad (23)$$

where the equality follows from the fact that $\Gamma_{S_i} > 0$ and $\Gamma_{S_j} > 0$, hence the left side term of the inequality in the expression within brackets is always non negative. Let us now consider the second term of the sum in Eqn. (22). We show that it goes to zero in the limit of μ_j going to infinity. Let us rewrite Eqn. (22) as follows:

$$Pr\left\{\frac{\Gamma_{S_j}}{\Gamma_{S_j}-\Gamma_{S_i}}\left(e^{-\frac{2^r-1}{\Gamma_{S_j}}}-e^{-\frac{2^r-1}{\Gamma_{S_i}}}\right) > R-e^{-\frac{2^r-1}{\Gamma_{S_i}}} \mid R-e^{-\frac{2^r-1}{\Gamma_{S_i}}} \geq 0\right\} Pr\left\{R-e^{-\frac{2^r-1}{\Gamma_{S_i}}} \geq 0\right\}$$

$$= Pr\left\{\frac{\Gamma_{S_j}}{\Gamma_{S_j}-\Gamma_{S_i}}\left(e^{-\frac{2^r-1}{\Gamma_{S_j}}}-e^{-\frac{2^r-1}{\Gamma_{S_i}}}\right) > \delta_i \mid \delta_i \geq 0\right\} Pr\left\{\delta_i \geq 0\right\}$$

$$= Pr\left\{\frac{\Gamma_{S_j}}{\Gamma_{S_j}-\Gamma_{S_i}}\left(e^{-\frac{2^r-1}{\Gamma_{S_j}}}-e^{-\frac{2^r-1}{\Gamma_{S_i}}}\right) > \delta_i \mid \delta_i \geq 0, \Gamma_{S_j} > \Gamma_{S_i}\right\} Pr\left\{\delta_i \geq 0 \mid \Gamma_{S_j} > \Gamma_{S_i}\right\} Pr\left\{\Gamma_{S_j} > \Gamma_{S_i}\right\}$$

$$+Pr\left\{\frac{\Gamma_{S_j}}{\Gamma_{S_j}-\Gamma_{S_i}}\left(e^{-\frac{2^r-1}{\Gamma_{S_j}}}-e^{-\frac{2^r-1}{\Gamma_{S_i}}}\right) > \delta_i \mid \delta_i \geq 0, \Gamma_{S_j} < \Gamma_{S_i}\right\} Pr\left\{\delta_i \geq 0 \mid \Gamma_{S_j} < \Gamma_{S_i}\right\} Pr\left\{\Gamma_{S_j} < \Gamma_{S_i}\right\},$$

$$(24)$$

where $\delta_i = R-e^{-\frac{2^r-1}{\Gamma_{S_i}}}$ is a r.v. that takes values in the interval $[0,+\infty)$. The first term of the sum in Eqn. (24) is the product of three probabilities. Recalling that $\gamma_j \sim exp(1)$ while $\Gamma_{S_j} = e^{\frac{X_j}{10}}$, for $j = 1,2$, with $X_j \sim \mathcal{N}(\mu_j, \sigma_j^2)$, we have:

$$Pr\left\{\Gamma_{S_j} > \Gamma_{S_i}\right\} = Pr\left\{e^{\frac{X_j}{10}} > e^{\frac{X_i}{10}}\right\} = Pr\left\{X_j > X_i\right\}$$

$$= \int_{-\infty}^{+\infty}\frac{1}{\sqrt{2\sigma_i^2}}e^{-\frac{(x_i-\mu_i)^2}{2\sigma_i^2}}\int_{x_i}^{+\infty}\frac{1}{\sqrt{2\sigma_j^2}}e^{-\frac{(x_j-\mu_j)^2}{2\sigma_j^2}}\,dx_j dx_i$$

$$= \int_{-\infty}^{+\infty}\frac{1}{\sqrt{2\sigma_i^2}}e^{-\frac{(x_i-\mu_i)^2}{2\sigma_i^2}}\left[\frac{1}{2}-\frac{1}{2}\text{erf}\left(\frac{x_i-\mu_j}{\sqrt{2\sigma_j^2}}\right)\right]dx_i, \quad (25)$$

where $\text{erf}(x)$ is the *error function*, defined as $\frac{2}{\sqrt{\pi}}\int_0^x e^{-t^2}dt$. Eqn. (25), under the hypotheses in the theorem statement, goes to 0 as $\mu_j \to -\infty$.

Let us now consider the second term of the sum in Eqn. (24). It can be easily shown that the first of the three probabilities that multiplied together compose such term goes to zero as

$\mu_j \to -\infty$. Let us call such term P_1. Then we have:

$$
\begin{aligned}
P_1 &= Pr\left\{ \frac{\Gamma_{S_j}}{\Gamma_{S_j} - \Gamma_{S_i}} \left(e^{-\frac{2^r - 1}{\Gamma_{S_j}}} - e^{-\frac{2^r - 1}{\Gamma_{S_i}}} \right) > \delta_i \,|\, \delta_i \geq 0, \Gamma_{S_j} < \Gamma_{S_i} \right\} \\
&= Pr\left\{ \left| \frac{\Gamma_{S_j}}{\Gamma_{S_j} - \Gamma_{S_i}} \right| \left| e^{-\frac{2^r - 1}{\Gamma_{S_j}}} - e^{-\frac{2^r - 1}{\Gamma_{S_i}}} \right| > \delta_i \,|\, \delta_i \geq 0, \Gamma_{S_j} < \Gamma_{S_i} \right\} \\
&\leq Pr\left\{ \frac{\Gamma_{S_j}}{\Gamma_{S_i} - \Gamma_{S_j}} \cdot R > \delta_i \,|\, \delta_i \geq 0, \Gamma_{S_j} < \Gamma_{S_i} \right\} \\
&= Pr\left\{ \Gamma_{S_j} > \Gamma_{S_i} \frac{\delta_i}{R(1 + \delta_i)} \,|\, \delta_i \geq 0, \Gamma_{S_j} < \Gamma_{S_i} \right\}.
\end{aligned} \tag{26}
$$

It can be shown in a similar way as in Eqn. (25) that (26) goes to zero asymptotically as μ_j goes to $-\infty$. Using equations (23)-(26) in Eqn. (7) we finally have:

$$
\begin{aligned}
\lim_{\mu_j \to -\infty} Pr\left\{ \frac{\Gamma_{S_1}}{\Gamma_{S_1} - \Gamma_{S_2}} e^{-\frac{2^r - 1}{\Gamma_{S_1}}} - \frac{\Gamma_{S_2}}{\Gamma_{S_1} - \Gamma_{S_2}} e^{-\frac{2^r - 1}{\Gamma_{S_2}}} > R \right\} &= Pr\left\{ e^{-\frac{2^r - 1}{\Gamma_{S_i}}} > R \right\} \\
&= \frac{1}{2} - \frac{1}{2}\mathrm{erf}\left(\frac{10 \ln\left[\frac{1 - 2^r}{\ln(R)} \right] - \mu_i}{2\sigma_i^2} \right).
\end{aligned} \tag{27}
$$

References

[1] European Telecommunications Standards Institute, "ETSI TS 102 584 V1.2.1, Digital Video Broadcasting (DVB); DVB-SH Implementation Guidelines Issue 2." Jan. 2011.

[2] Exalted Project, "First report on LTE-M algorithms and procedures," http://www.ict-exalted.eu, Aug. 2011.

[3] T. M. Cover and J. A. Thomas, *Elements of Information Theory*, second edition ed. John Wiley & Sons, 2006.

[4] D. S. Lun, M. Médard, R. Koetter, and M. Effros, "On coding for reliable communication over packet networks," *Physical Comm.*, vol. 1, no. 1, pp. 3–20, 2008. [Online]. Available: http://www.sciencedirect.com/science/article/pii/S1874490708000086

[5] J. Laneman, D. Tse, and G. Wornell, "Cooperative diversity in wireless networks: Efficient protocols and outage behavior," *IEEE Trans. on Info. Theory*, vol. 50, no. 12, pp. 3062–3080, Dec. 2004.

[6] Y. Tseng, S. Ni, Y. Chen, and J. Sheu, "The broadcast storm problem in a mobile ad hoc network," *Wireless Networks*, vol. 8, pp. 153–167, 2002.

[7] J. Wu and F. Dai, "A generic distributed broadcast scheme in ad hoc wireless networks," *IEEE Trans. on Computers*, vol. 53, no. 10, pp. 1343–1354, Oct. 2004.

[8] A. Vanelli-Coralli, G. E. Corazza, G. K. Karagiannidis, P. T. Mathiopoulos, D. S. Michalopoulos, C. Mosquera, S. Papaharalabos, and S. Scalise, "Satellite communications: Research trends and open issues," in *Int'l Workshop on Satellite and Space Comm.*, Toulouse, France, Sept. 2007.

[9] S. Morosi, E. D. Re, S. Jayousi, and R. Suffritti, "Hybrid satellite/terrestrial cooperative relaying strategies for DVB-SH based communication systems," in *European Wireless Conf.*, Aalborg (Denmark), May 2009.

[10] G. Cocco, C. Ibars, and O. D. R. Herrero, "Cooperative satellite to land mobile gap-filler-less interactive system architecture," in *IEEE Advanced Satellite Mobile Systems Conf.*, Cagliari, Italy, Sep. 2010.

[11] T. Ho, M. Médard, R. Koetter, D. R. Karger, M. Effros, J. Shi, and B. Leong, "A random linear network coding approach to multicast," *IEEE Trans. on Info. Theory*, vol. 52, no. 10, pp. 4413–4430, Oct. 2006.

[12] P. A. Chou, Y. Wu, and K. Jain, "Practical network coding," in *IEEE Allerton Conf. on Communication, Control, and Computing*, Urbana-Champaign, IL, U.S.A., Oct. 2003.

[13] R. Ahlswede, C. Ning, S.-Y. R. Li, and R. W. Yeung, "Network information flow," *IEEE Trans. on Info. Theory*, vol. 46, no. 4, pp. 1204–1216, July 2000.

[14] M. Sardari, F. Hendessi, and F. Fekri, "Infocast: A new paradigm for collaborative content distribution from roadside units to vehicular networks," in *Annual IEEE Comm. Society Conf. on Sensor, Mesh and Ad Hoc Comm. and Networks*, Rome, Italy, June 2009.

[15] P. Cataldi, A. Tomatis, G. Grilli, and M. Gerla, "A novel data dissemination method for vehicular networks with rateless codes," in *IEEE Wireless Comm. and Networking Conf. (WCNC)*, Budapest, Hungary, Apr. 2009.

[16] S. Sreng, B. Escrig, and M.-L. Boucheret, "Exact symbol error probability of hybrid/integrated satellite-terrestrial cooperative network," *Wireless Communications, IEEE Transactions on*, vol. 12, no. 3, pp. 1310–1319, March 2013.

[17] M. Arti and M. Bhatnagar, "Beamforming and combining in hybrid satellite-terrestrial cooperative systems," *IEEE Communications Letters*, vol. PP, 2014.

[18] M. Bhatnagar and M. Arti, "Performance analysis of af based hybrid satellite-terrestrial cooperative network over generalized fading channels," *IEEE Communications Letters*, vol. 17, no. 10, pp. 1912–1915, Oct. 2013.

[19] G. Cocco, C. Ibars, and N. Alagha, "Cooperative coverage extension in heterogeneous Machine-to-Machine networks," in *Globecom 2012 Workshop: Second International Workshop on Machine-to-Machine Communications 'Key' to the Future Internet of Things*, Anaheim, CA, U.S.A., Dec. 2012.

[20] G. Cocco, N. Alagha, and C. Ibars, "Network-coded cooperative extension of link level FEC in DVB-SH," in *AIAA International Communications Satellite Systems Conf.*, Nara, Japan, Dec. 2011.

[21] D. Jiang and L. Delgrossi, "IEEE 802.11p: Towards an international standard for wireless access in vehicular environments," in *IEEE Vehicular Technology Conference (VTC Spring)*, Korea, Seoul, May 2008.

[22] H. Himmanen, "Studies on channel models and channel characteristics for mobile broadcasting," in *IEEE International Symposium on Broadband Multimedia Systems and Broadcasting*, Las Vegas, NV, U.S.A., Mar. 2008.

[23] European Telecommunications Standards Institute, "ETSI TS 102 584 V1.2.1 DVB-SH Implementation Guidelines; Technical Specifications," http://www.etsi.org/, Jan. 2011.

[24] L. Wan, S. Tsai, and M. Almgren, "A fading-insensitive performance metric for a unified link quality model," in *IEEE Wireless Comm. and Networking Conf.*, vol. 4, Las Vegas, NV, U.S.A., Apr. 2006.

[25] Sony, Intel, "TGn sync proposal MAC simulation methodology," IEEE 21 802.11-04/895r2, Nov. 2004.

[26] "Draft IEEE 802.16m evaluation methodology." http://www.ieee802.org/16/tgm/docs/80216m-07_037r2.pdf: Institute of Electrical and Electronics Engineers (IEEE), Dec. 2007.

[27] F. Kaltenberger, I. Latif, and R. Knopp, "On scalability, robustness and accuracy of physical layer abstraction for large-scale system-level evaluations of LTE networks," in *Asilomar Conference on Signals, Systems and Computers*, Pacific Groove, CA, U.S.A., Nov. 2013.

[28] C. Meng, H. Wang, W. Heng, and J. Zhang, "Physical layer abstraction algorithm based on RBIR for CDMA EVDO and WLAN," in *International Conference on Wireless Communications and Signal Processing*, Nanjing, China, Nov 2011.

[29] *ANSI/IEEE Std 802.11, 1999 Edition (R2003)*, Institute of Electrical and Electronics Engineers (IEEE), http://ieeexplore.ieee.org/xpl/mostRecentIssue.jsp?punumber=9543, 1999.

[30] S. Deb, M. Effros, T. Ho, D. R. Karger, R. Koetter, D. S. Lun, M. Mdard, and N. Ratnakar, "Network coding for wireless applications: A brief tutorial," in *IEEE Int'l Workshop on Wireless Ad-hoc Networks*, London, UK, May 2005.

[31] H. Suzuki, "A statistical model for urban radio propogation," *IEEE Trans. on Comm.*, vol. 25, no. 7, pp. 673–680, July 1977.

[32] E. Lutz, D. Cygan, M. Dippold, F. Dolainsky, and W. Papke, "The land mobile satellite communication channel-recording, statistics, and channel model," *IEEE Trans. on Vehicular Technology*, vol. 40, no. 2, pp. 375–386, May 1991.

[33] F. Perez-Fontan, M. A. Vazquez-Castro, S. Buonomo, J. P. Poiares-Baptista, and B. Arbesser-Rastburg, "S-band LMS propagation channel behaviour for different environments, degrees of shadowing and elevation angles," *IEEE Trans. on Broadcasting*, vol. 44, no. 1, pp. 40–76, Mar. 1998.

[34] "Digital Video Broadcasting (DVB); Upper Layer Forward Error Correction in DVB. DVB Document A148," http://www.dvb.org/, Mar. 2010.

[35] European Telecommunications Standards Institute, "ETSI TS 102 472 V1.1.1, Digital Video Broadcasting (DVB); IP Datacast over DVB-H: Content Delivery Protocols," June 2006.

[36] I. Sen and D. W. Matolak, "Vehicle-vehicle channel models for the 5-GHz band," *IEEE Trans. on Intelligent Transportation Systems*, vol. 9, no. 2, pp. 235–245, June 2008.

[37] G. Acosta-Marum and M. A. Ingram, "Six Time- and Frequency-Selective Empirical Channel Models for Vehicular Wireless LANs," in *IEEE Vehicular Technology Conf.*, Baltimore, MD , U.S.A., Sept. 2007.

[38] G. Acosta, K. Tokuda, and M. A. Ingram, "Measured joint Doppler-delay power profiles for vehicle-to-vehicle communications at 2.4 GHz," in *IEEE Global Telecomm. Conf.*, Dallas, TX, U.S.A., Nov. 2004.

[39] L. Cheng, B. E. Henty, , D. D. Stancil, F. Bai, and P. Mudalige, "Mobile vehicle-to-vehicle narrow-band channel measurement and characterization of the 5.9 GHz dedicated short range communication (DSRC) frequency band," *IEEE Journal on Selected Areas in Comm.*, vol. 25, no. 8, pp. 1501–1516, Oct. 2007.

[40] COST207, "Digital land mobile radio communications (final report)," Commission of the European Communities, Directorate General Communications, Information Industries and Innovation, Tech. Rep., 1989.

[41] Y. C. Cheng, J. Bellardo, P. Benkö, A. C. Snoeren, G. M. Voelker, and S. Savage, "Jigsaw: Solving the puzzle of enterprise 802.11 analysis," in *Special Interest Group on Data Comm. Conf.*, Pisa, Italy, Sep. 2006.

[42] J. Lei, M. A. Vazquez-Castro, and T. Stockhammer, "Link-layer FEC and cross-layer architecture for DVB-S2 transmission with QoS in railway scenarios," *IEEE Trans. on Vehicular Technology*, vol. 58, no. 8, pp. 4265–4276, Oct. 2009.

[43] European Telecommunications Standards Institute, "ETSI EN 302 583 V 1.2.1, Digital Video Broadcasting (DVB); Framing Structure, channel coding and modulation for Satellite Services to Handheld devices (SH) below 3 GHz." Ago. 2008.

[44] F. Vieira and J. Barros, "Network coding multicast in satellite networks," in *Conf. on Next Generation Internet Networks*, Aveiro (PO), July 2009.